Verification studies of a simplified model for the removal of dichloromethane from waste gases using a biological trickling filter (Part I)

Bioprocess Engineering 6 (1991) 93–99
0178515X91000027

Bioprocess Engineering

Verification studies of a simplified model for the removal of dichloromethane from waste gases using a biological trickling filter

(Part I) *

R. M. M. Diks and **S. P. P. Ottengraf,** Eindhoven

Abstract. The removal of dichloromethane from waste gases in a biological trickling filter was studied experimentally as well as theoretically within the concentration range of 0–10,000 ppm. A stable dichloromethane elimination performance was achieved during two years of operation, while the start-up of the system only amounted to several weeks at constant inlet concentrations. The trickling filter system was operated co-currently as well as counter-currently.

However, experimental and theoretical results revealed that the relative flow direction of the mobile phases did not significantly affect the elimination performance. Moreover, it was found that the gas-liquid mass-transfer resistance in the trickling filter bed applied was negligible, which leaves the biological process inside the biofilm to be the rate limiting step.

A simplified model was developed, the "Uniform-Concentration-Model", which showed to predict the filter performance close to the numerical solutions of the model equations. This model gives an analytical expression for the degree of conversion and can thus be easily applied in practice.

The dichloromethane eliminating performance of the trickling filter described in this paper, is reflected by a maximum dichloromethane elimination capacity $EC_{max} = 157$ g/(m³ · h) and a critical liquid concentration $C_{lcr} = 45$ g/m³ at a superficial liquid velocity of 3.6 m/h, inpendent of the gas velocity and temperature.

List of symbols

a_s	m²/m³	specific area
a_w	m²/m³	specific wetted area
A	m²	cross-sectional area
C_g	g/m³	gas phase concentration
C_{go}	g/m³	inlet gas phase concentration
$C_{g_{ocr}}$	g/m³	critical gas phase concentration
C_g^*	–	$\frac{C_g}{C_{go}}$ dimensionless gas concentration
C_l	g/m³	liquid concentration
C_{lcr}	g/m³	critical liquid concentration
C_{lcr}^*	–	$\frac{m C_{lcr}}{C_{go}}$ dimensionless critical concentration
C_{li}	g/m³	substrate concentration at liquid-biofilm interface
C_l^*	–	$\frac{m C_l}{C_{go}}$ dimensionless liquid concentration
C_o	g/m³	oxygen concentration inside the biofilm
C_{oi}	g/m³	oxygen concentration at liquid-biofilm interface
C_s	g/m³	substrate concentration inside the biofilm
C_{si}	g/m³	substrate concentration at liquid-biofilm interface
D_{eff}	m²/h	effective diffusion coefficient in the biofilm
D_o	m²/h	effective diffusion coefficient for oxygen in the biolayer
E	–	$\frac{m u_g}{u_l}$ extraction factor
E_{act}	kJ/mol	activation energy for the biological reaction
EC	g/(m³ · h)	$K_o a_w \delta \eta$: elimination capacity, or the amount of substrate degraded per unit of reactor volume and time
EC_{max}	g/(m³ · h)	$K_o a_w \delta$: maximum elimination capacity
f	–	degree of conversion
h	m	coordinate in height
H	m	height of the packed bed
K_0	g/(m³ · h)	$\frac{\mu_{max} X_b}{Y}$ zeroth order reaction defined per unit of biofilm volume
k_{og}	m/h	overall gas phase mass transfer coefficient
K^*	–	dimensionless constant given by Eq. (A.5)
K_1^*	–	dimensionless constant given by Eq. (A.6)
K_2^*	–	dimensionless constant given by Eq. (A.6)
m	–	$\frac{C_g}{C_l}$ gas liquid distribution coefficient
N	g/(m² · h)	liquid-biofilm interfacial flux of substrate
N_{og}	–	$\frac{k_{og} a_w H}{u_g}$ number of gas phase transfer units
N_r	–	$\frac{K_o a_w \delta H}{u_g C_{go}}$ number of reaction units
OL	g/(m³ · h)	$\frac{u_g C_{go}}{H}$ organic load
r_s	g/(m³ · h)	zeroth order substrate degradation rate given by Eq. (1)
R_s	g/(g TSS · h)	specific activity
T	K	absolute temperature
u_g	m/h	superficial gas velocity
u_l	m/h	superficial liquid velocity
X_b	g TSS/m³	biomass concentration inside biofilm
X_s	g TSS/m³	liquid suspended biomass concentration
x	m	coordinate inside the biofilm
Y	g TSS/(g_{DCM})	yield coefficient

* Experimental results, verifying the model presented will be discussed in Part II (to be published in Vol. 6, No. 4)

Greek symbols

Γ	–	dimensionless parameter given by Eq. (2)
δ	m	averaged biofilm thickness
η	–	biofilm effectiveness factor given by Eqs. (7a)–(7c)
Λ	m	penetration depth of substrate into the biofilm
μ_{max}	d^{-1}	microbiological maximum growth rate
ν_o	–	stoichiometric utilization coefficient for oxygen
ν_s	–	stoichiometric utilization coefficient for substrate
ξ	–	dimensionless height in the filter bed
τ	h	$\frac{H}{u_g}$ superficial gas phase contact time
Φ_0	–	$\delta\left(\frac{K_0}{D\,C_{li}}\right)^{1/2}$
ψ_0	–	$\frac{C_o}{C_{oi}}$ dimensionless oxygen concentration inside the biofilm
ψ_s	–	$\frac{C_s}{C_{si}}$ dimensionless substrate concentration inside the biofilm

1 Introduction

In the last decade the biological treatment of waste gases has become an important alternative to many physical- and physico-chemical methods of exhaust gas purification. The number of applications has increased, especially for the removal of odorous, easily biodegradable compounds e.g. in the food processing industry, flavour and fragrance industry, sewage treatment works etc. [1–4]. This technique has proved to lend itself not only to the reduction of odour emissions, but also to the prevention of air contamination with undesirable xenobiotic compounds in general, which are discharged e.g. by the chemical industry [5, 6].

Due to intensive microbiological research in recent years, micro-organisms, mainly bacteria, have been isolated and selected, which show an activity and stability to such an extent, that the practical use in biological waste gas treatment systems offers real prospects by this time.

For example dichloromethane was still regarded as non-biodegradable in 1980 [7], but ever since literature has been published, describing bacteria like Hyphomicrobium sp. or Pseudomonas sp., that are able to use this compound as their sole carbon- and energy source [8–16], with sufficiently high growth rates.

Increasing attention is paid to biological waste gas purification processes due to some important advantages this technique has over conventional purification methods. Apart from the mild conditions applied (low pressure and temperature), biological degradation processes do not generally shift the pollution problem towards another environmental compartment (gas into solid, solid into water etc.), which is often characteristic for many other purification methods. Biological treatment is especially effective in the lower concentration range (ppm level), which is often encountered in cases of odorous or toxic waste gas emissions. Moreover, it is relatively cheap as compared to e.g. adsorption or combustion [17]. Among the biological waste gas treatment systems, biofilters have the widest application [6]. They consist of a simply structured packed bed, in which the gas flow is intensively contacted with an immobilized microbial flora [4, 18]. Problems of inhibition may however rise, if during the degradation process acid metabolites are produced to such an extent, that pH buffering of the packing material is only effective for a relatively short period of operation [2, 20]. This is mainly the case during the degradation of halogenated hydrocarbons, where acids are produced.

In these cases the use of a biological trickling filter is favourable, because the recirculated water phase in this system allows the continuous neutralization of the acids produced, as well as the drainage of neutralization products [5, 19, 20].

This paper aims to present the results of an investigation of dichloromethane removal from waste gases in a biological trickling filter. It is commonly thought, that the application of these trickling filters is restricted only to compounds which show good or at least moderate water solubility [17, 21]. For dichloromethane, being poorly water-soluble, it is shown that the biological reaction instead of the gas-liquid mass transfer is the rate-limiting step. Nevertheless, high degrees of conversion can be reached. Dichloromethane is used in huge quantities in many sorts of industrial activity [22, 23]. Because of its suspected carcinogenic properties, the maximum allowable gas concentration for emission is 150 mg/m^3, according to the German TA-luft [24]. However, industrial emissions of dichloromethane generally take place on much higher concentration levels ranging up to 10,000 mg/m^3 [22].

In this study the experimental results of a two-year investigation are presented, including a simplified model which describes the elimination performance of a trickling filter in relation to the process variables of practical interest. This model may also be used as a basis for full-scale biological trickling filter design.

2 Experimental

2.1 Experimental set-up

Experiments to study the degradation of dichlormethane were carried out in a continuously operating lab-scale trickling filter bed. The installation, schematically shown in Fig. 1, consisted of a cylindrical glass fiber reinforced plastic column, with a diameter of 0.40 m and a height of 4 m. The height of the packing was 2.7 m, and sampling points for both gas and liquid were present at intervals of 0.5 m. The packing material consisted of ½″ keramic Novalox saddles (VFF GmbH & Co., W-Germany), with a specific packed interfacial area of 750 m^{-1}. The resulting void volume amounted to 68%.

The waste gas was introduced either at the bottom or at the top of the column, in order to investigate counter-current

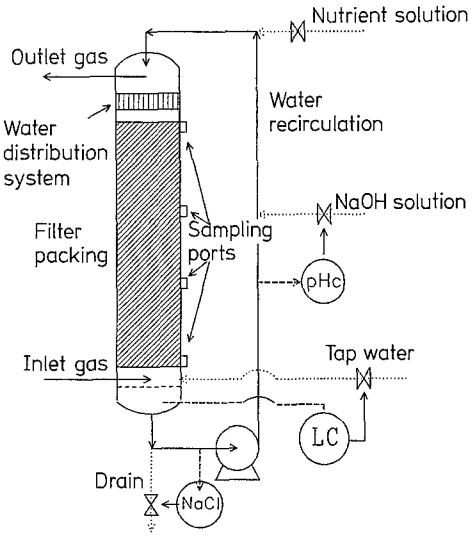

Fig. 1. Experimental set-up of the biological trickling filter system

as well as co-current operation. The waste gas was created by continuously dosing liquid dichloromethane into an airflow. The storage vessel of dichloromethane was connected to a capillary with a length of 3 m and an inner diameter of 0.3 mm. By pressurizing the storage vessel a known and constant flow of dichloromethane was produced. The injection took place in a flange with a central opening of 10 mm. Due to the high gas velocity immediate evaporation of the dichloromethane took place. In this way concentrations ranging from 500 mg/m^3 up to 10,000 mg/m^3 could be produced.

The water phase was continuously recirculated and distributed over the bed, using a Veiki distribution system (Polarcel, The Netherlands), consisting of three polyethylene decks, which are formed of a rectangular network of slats (the distance between the slats is 40 mm, the height of a slat is 18 mm). To provide a uniform distribution of water over the deck, each individual slat is grooved on top. An important advantage of this distributor is the negligible pressure drop, and the absence of blocking by the biomass present in the water phase (as occurs with nozzles). The superficial water velocity was varied from 1.8 to 11 (m^3/m^2 · h). The minimum wetting rate for the packing was about 8 m/h. The liquid from the filterbed was collected at the bottom, and recirculated to the top of the column.

In the liquid volume under the filterbed the pH of the liquid phase was controlled (Radiometer, Denmark) by dosing an alkaline solution (5 M NaOH, Merck), to neutralize the hydrochloric acid which is formed during the biological dichloromethane degradation. From the amount of NaOH-solution dosed per unit time, the conversion rate or elimination capacity can be calculated. Two pH-electrodes were incorporated in the system. One was connected to the pH-control apparatus, and the other electrode was used to secure the system against extreme pH-values. In case of disturbances (pH < 5 or pH > 9), the supply of both dichloromethane and NaOH-solution were shut off, to protect the biological activity. The temperature of the liquid phase was controlled using a heat exchanger, which was placed in the recirculation conduit.

As a high concentration of neutralization products (viz. NaCl) inhibits the biological activity [2, 9, 10, 20], a continuous drain of liquid from the reactor took place. In order to maintain the required level of inorganic nutrients, a concentrated nutrient solution was fed to the reactor. The additional water supply, to compensate for the drain and evaporation, was controlled by an automatic level controller.

2.2 Materials and methods

Bacterial culture. The strain Hyphomicrobium sp., GJ21, [10], was used for the degradation of dichloromethane. At a pH = 7.5–7.7 and a temperature of 20°–22°, the maximum growth rate of this organism is 2.6 d^{-1}, and the Monod constant amounts to 3 μM [25]. The yield of biomass on dichloromethane is 0.17 gram dry weight biomass formed per gram of dichloromethane degraded. The specific activity of the biomass at dichloromethane concentrations exceeding the Monod constant can be calculated as the ratio of the μ_{max} and the yield coefficient Y. For the pure culture of Hyphomicrobium sp., the specific activity amounts to 0.64 g dichloromethane/g TSS, h.

Growth and maintenance of bacteria. The mineral medium for batch growth experiments was composed following Janssen et al. [26]. This medium contains a high phosphate concentration, in order to neutralize the acids produced.

In the pilot plant experiments the medium was based on tap water, which had a composition comparable to the medium for batch experiments, with respect to all spore elements. Additions were necessary only of phosphate (0.25 g/dm^3 K_2HPO_4), ammonium (1 g/dm^3 $(NH_4)_2SO_4$), and iron (1 mg/dm^3 $FeSO_4 \cdot 6\,H_2O$). Both ammonium and phosphate concentrations were related to the quantity of carbon converted into biomass using the general biomass composition formula $C_5H_7NO_2P_{1/30}$.

Additional conditions. In the pilot plant the temperature was maintained at 20 °C or 30 °C, while the pH of the liquid entering the filter bed was maintained at a value of 8 to prevent the occurrence of low pH values in the lower part of the system, due to acidification along the height of the filter.

The concentration of NaCl in the filter system, which was kept at a constant level of 100 mM to avoid inhibiting effects, was recorded by continuous measurement of the electrical conductivity of the liquid phase.

Analysis. Dichloromethane concentrations were determined on a Carlo Erba 4300 gas chromatograph provided with a 3 cm^3 gas sample loop and a flame ionization detector. A 30% PEG column of 1 m was used at 100 °C, at a carrier gas flow rate of 30 cm^3/min. From the inlet- and outlet gas phase concentrations the degree of conversion was thus determined, which was checked by calculating the ratio of the amount of dichloromethane used and the amount of NaOH-solution dosed over a certain period of time.

The liquid dichloromethane concentration was analysed using the so-called headspace technique. Samples of 9 cm^3 were taken into 13 cm^3 vials. After closing with a Viton-rubber cap, the vials were thermostatted at 30 °C for 30 min with regular shaking. After equilibrium had been reached, a 250 µl gas sample was directly injected into the chromatograph. All analyses were carried out in duplo.

Total suspended solids. The concentration of biomass, which is expressed as the total amount of suspended solids, was determined by filtration. The biomass of a liquid sample was collected on a glass fiber filter (∅ 47, No. 6; Schleicher & Schüll, W.-Germany). After washing with destilled water, the filter was dried at 60 °C.

3 Theoretical model

In the following a theoretical model is presented, which describes the elimination capacity of a trickling filter system eliminating a carbon source introduced by the gas phase. In the model the intrinsic kinetics as well as the transport phenomena are taken into consideration. The substrate is transferred to the liquid phase, which runs over the biofilm formed on the packing material. In the biofilm the overall process is regarded as the result of a combination of transport by diffusion and a biological reaction. Because of the complexity of the system, simplification is achieved using the following assumptions [27–29]:

1) a steady state situation is assumed in the filter system, which implies the presence of a biofilm, that has a constant thickness, activity and contact area, independent of time;

2) the biological reaction kinetics inside the biofilm are of zeroth order in the substrate concentration. This means that the Monod constant is sufficiently small compared to the substrate concentration. Theoretical considerations as well as experimental results reviewed by Härremoes [30] show that the zeroth order assumption is valid for $C_l > 5\,K_s$. For the degradation of dichloromethane this means that the liquid concentration should exceed a value of 1.3 mg/dm^3 [25, 44]. At 20 °C this corresponds to an equilibrium gas phase concentration of 145 mg/m^3. As inlet gas concentrations in practice are mostly above this level, the assumption is acceptable. The zeroth order substrate degradation rate is thus given by

$$r_s = \frac{\mu_{\max} X_b}{Y} = K_0; \tag{1}$$

3) intrinsic kinetic parameters determined in batch are still valid for the immobilized biofilm system;

4) the biomass concentration X_b inside the biolayer is constant, which means that growth only results in an increase of the biofilm thickness. However, a certain biofilm thickness is maintained, due to decay and sloughing;

5) the biofilm thickness δ is small as compared to the characteristic size d_p of the coated packing elements in the filter bed, hence the biofilm may be regarded as a flat slab;

6) the attached biofilm is a separate phase from the flowing liquid, and interfacial mass transfer resistance in the liquid near the biofilm may be neglected. Both aspects have been investigated and confirmed by Atkinson et al., for biofilms converting glucose in a flat-film reactor as well as a packed bed reactor [31, 32];

7) the substrate degradation reaction only takes place inside the biofilm itself, i.e. substrate degradation in the flowing liquid phase can be neglected due to the very low biomass concentration present in this phase;

8) the substrate supplied via the gas phase is the only carbon- and energy source;

9) no oxygen limitation is thought to occur throughout the substrate concentration range indicated. The importance of oxygen limitation can be estimated theoretically by comparing the substrate availability and the rate of reaction for oxygen as well as dichloromethane, which are closely bound up with the stoichiometry of the overall reaction equation. This relationship is given in Eq. (2) [33]:

$$\Gamma \frac{d^2\psi_o}{dx^2} = \frac{d^2\psi_s}{dx^2}, \tag{2}$$

where

$$\psi_o = \frac{C_o}{C_{oi}}; \quad \psi_s = \frac{C_s}{C_{si}}; \quad \Gamma = \frac{D_o\, v_s\, C_{oi}}{D_{\text{eff}}\, v_o\, C_{si}}.$$

In these equations, D_{eff} and D_o are the effective diffusion coefficients in the biofilm; v_s, v_o are the utilization coefficients, and C_{oi}, C_{si}, C_o and C_s are the oxygen- and substrate concentration at the biofilm interface, and the inner biofilm, respectively. For any reaction order substrate limitation will occur if $\Gamma > 1$. Oxygen limitation will occur for $\Gamma < 1$ [33]. As for the system dichloromethane-oxygen $D_o/D_{\text{eff}} = 2$, $v_s/v_o = 3$ mg dichloromethane/mg oxygen, and $C_{oi} = 8.5$ mg/dm^3 ($T = 20$ °C), oxygen limitation inside the biofilm occurs according to Eq. (2) at dichloromethane concentrations in the liquid phase above 51 mg/dm^3, which corresponds with equilibrium gas phase concentrations above 6 g/m^3;

10) both gas and liquid phases are in plug flow, i.e. no longitudinal mixing, due to channelling, diffusion or velocity distribution, occurs.

With the above-presented assumptions a physico-mathematical description of the trickling filter is given below. Intrinsic kinetics are of zeroth order, as discussed previously.

The system modelling is carried out in two steps: firstly transversal concentration profiles and interfacial fluxes in the biolayer are calculated at an arbitrary height in a cross section of the column. Secondly the overall performance of the reactor is calculated by integrating the differential equations describing the axial concentration profiles in the gas and the liquid phase.

For a reaction taking place in a biolayer, two situations can be distinguished, according to Ottengraf [27]. In case of high interfacial concentrations the limiting process inside the biolayer will be the rate of the biological reaction itself. This

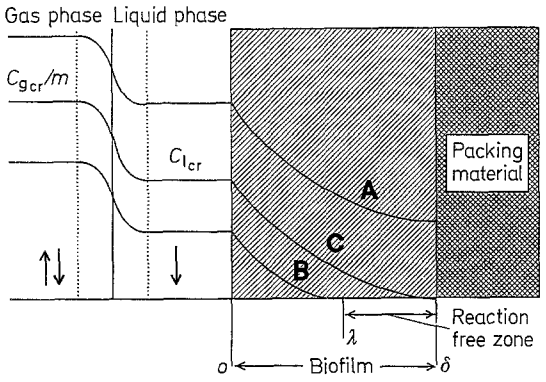

Fig. 2. Biophysical model for the trickling filter system. Concentration profiles inside the biofilm: reaction limitation (*A*); diffusion limitation (*B*); critical gas and liquid concentration (*C*)

implies the biofilm to be fully penetrated with substrate, as illustrated by curve A in Fig. 2.

For this situation the concentration profile inside the biolayer and the interfacial flux are given by [27]:

$$\frac{C_s}{C_{si}} = 1 + \frac{\Phi_0^2}{2}(\sigma^2 - 2\sigma), \tag{3}$$

$$N = -\frac{D_{\text{eff}}}{\delta}\left(\frac{dC_{si}}{d\sigma}\right)_{\sigma=0} = K_0\,\delta \tag{4}$$

with

$$\Phi_0 = \delta\left(\frac{K_0}{D_{\text{eff}}\,C_{si}}\right)^{1/2} \quad \text{(zeroth order Thiele number).}$$

At lower interfacial concentrations (curve B), Fig. 2) the respective magnitudes are given by:

$$\frac{C_s}{C_{si}} = 1 + \frac{\Phi_0^2}{2}\left(\sigma^2 - 2\sigma\frac{\lambda}{\delta}\right); \tag{5}$$

$$N = -\frac{D_{\text{eff}}}{\delta}\left(\frac{dC_{si}}{d\sigma}\right)_{\sigma=0} = K_0\,\lambda. \tag{6}$$

The reaction free zone shown in Fig. 2 occurs due to zeroth order kinetics.

As no mass transfer resistance is present in the liquid near the biofilm, C_{si} equals C_{li}. If the effectiveness of the biofilm is defined as the ratio of the actual flux and the maximum flux at reaction controlled conditions, it follows from Eqs. (3)–(6):

$$\eta = 1 \qquad \text{for} \quad \Phi_0 \leqq \sqrt{2}; \tag{7a}$$

$$\eta = \frac{\lambda}{\delta} = \left(\frac{C_{li}}{C_{lcr}}\right)^{1/2} \qquad \text{for} \quad \Phi_0 \geqq \sqrt{2}, \tag{7b}$$

with

$$C_{lcr} = \frac{K_0\,\delta^2}{2D_{\text{eff}}}. \tag{7c}$$

In order to calculate the axial gas and liquid concentration profiles two modes of operation concerning the relative flow direction of both phases can be distinguished: counter-current and co-current flow.

If plug flow conditions of the gas phase are assumed, it follows from a differential mass balance for the gas phase concentration:

$$-u_g\left(\frac{dC_g}{dh}\right) = \pm\, k_{og}\,a_w(C_g - m\,C_l) \tag{8}$$

or in dimensionless notation:

$$\left(\frac{dC_g^*}{d\xi}\right) = \pm\, N_{og}(C_g^* - C_l^*), \tag{9}$$

where the + sign refers to co-current and the − sign to counter-current operation.

If the liquid flow is also considered to be of the plug flow type, its substrate concentration is given by:

$$-u_l\left(\frac{dC_l}{dh}\right) = k_{og}\,a_w(C_g - m\,C_l) - K_0\,\delta\,a_s\,\eta \tag{10}$$

or with dimensionless parameters

$$\left(\frac{dC_l^*}{d\xi}\right) = -E N_{og}(C_g^* - C_l^*) + N_r\,\eta. \tag{11}$$

In Eq. (10) $K_0 \cdot \delta \cdot a_w$ equals the maximum elimination capacity $EC_{\max}$ of a filter bed defined as the maximum amount of substrate degraded per unit of reactor volume and time, which is frequently used to express the filter performance.

The boundary conditions belonging to Eqs. (9) and (11) are:

$$\xi = 0: \quad C_g^* = 1 \quad \text{for counter-current flow,} \tag{12a}$$

$$\xi = 1: \quad C_g^* = 1 \quad \text{for co-current flow} \tag{12b}$$

and

$$C_l^*(0) = C_l^*(1). \tag{12c}$$

The boundary condition according to Eq. (12c) accounts for the recirculation of the liquid phase, and denotes that no substrate removal is assumed in the liquid phase outside the filter bed.

As the mass transfer resistance in the liquid film near the biofilm interface is neglected, the interfacial biofilm concentration C_{li} equals the bulk liquid concentration C_l, which allows to express the biofilm effectiveness factor η as a function of C_l according to Eq. (7b).

A set of non-linear differential equations has now been obtained, for which no analytical solution exists. Numerical procedures have been applied to solve this problem. Calculations were carried out on a PC in Turbo-Pascal, using a fifth-order Runge-Kutta procedure, together with a procedure called ZEROINAB, to solve iteratively for the boundary condition given by Eq. (12c).

Some calculated axial gas and liquid concentration profiles are shown in Fig. 3a and b. It should be emphasized hat

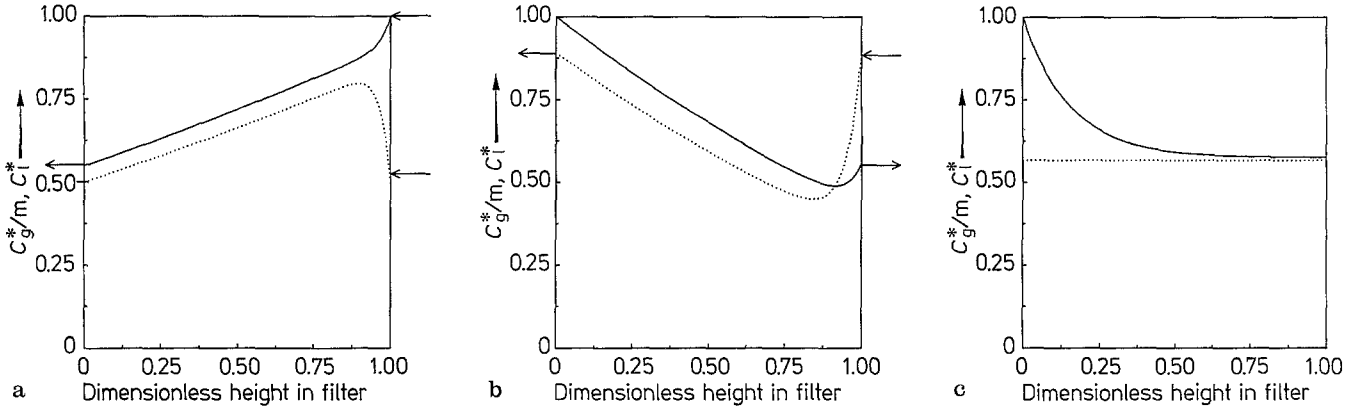

Fig. 3a–c. Axial gas (solid line) and liquid (dotted line) concentration profiles for co-current flow **(a)**, counter-current flow **(b)** and UCM-model **(c)**. $N_r=0.71$; $E=3.78$; $C^*_{lcr}=1.64$; $N_{og}=6$

according to the theoretical results presented in this figure, counter-current operation allows the occurence of stripping in the upper part of the trickling filter. This phenomenon, which of course is very disadvantageous, can be explained by the intensive contact between the gas and liquid phases. As a result the concentration in the liquid (C_{l0}) leaving the filter bed approaches a value which is in equilibrium with the inlet gas phase concentration (C_{g0}/m).

Due to the recirculation of this liquid to the top of the column there is supersaturation with respect to the outlet gas, thus causing the stripping effect.

In order to restrict the number of experiments, calculations have been made comparing co- and counter-current flow operation as described, which show the most important features and characteristics of both models. These calculations include the elimination capacity versus the inlet gas concentration, as well as the axial gas and liquid concentration profiles. Value ranges of parameters and corresponding dimensionless numbers applied in these calculations are listed in Table 1. They reflect the range of practical interest for the system dichloromethane-water. Physical constants and mass transfer data presented in Table 1 have been obtained from literature [34–37], kinetic data from this study.

Co-current flow was expected to give better results in the diffusion limited regime, because of the lack of stripping effects. However, analysis of the numerical results shows that the performance of the trickling filter is hardly influenced by the flow direction of the mobile phases. Only small differences show to exist throughout the parameter ranges indicated in Table 1; deviations are smaller at lower degrees of conversion.

This phenomenon can be explained by the smoothing effect the recirculation of the liquid phase has on the axial concentration profile, thus reducing the axial concentration gradients in the liquid phase. As the conversion rate depends on the square root of the liquid concentration according to Eq. (7b), it will be clear that differences of the local conversion rate are increasingly reduced.

It can be concluded that the overall filter efficiency, although depending on the local liquid concentration, will be determined to a minor extent by the path of the axial concentration profile.

Table 2 lists the overall degrees of conversion reached after the gas phase has passed each stage of a number of successive trickling filters, each with its own water recircula-

Table 1. Dimensionless parameters as calculated from practical values of the process parameters for dichloromethane [34–37]

Dimensioned parameters				Dimensionless parameters	
EC_{max}	= 100 – 300	$g/(m^3 \cdot h)$		N_r	= 0.03 – 150
C_{lcr}	= 12 – 75	g/m^3		N_{og}	= 0.3 – 8.3
u_g	= 80 – 500	m/h		E	= 0.8 – 44
u_l	= 1.8 – 10.8	m/h		C^*_{lcr}	= 0.09 – 119
C_{go}	= 0.1 – 15	g/m^3			
m	= 0.1 – 0.15				
A	= 0.125	m^2			
$k_{og}a_w$	= 0.001 – 0.1	s^{-1}			

Table 2. The degree of conversion reached in a series of trickling filters; $N_r=44.6\,\tau$; $N_{og}=400\,\tau$ (τ in h); $\tau_{total}=n\,\tau_{stage}$; $C^*_{lcr}=1.64$; $E=0.0153\,u_g$ (u_g in m/h)

Mode of operation	u_g [m/h] per stage	H [m]	τ [10^{-3} h]	Degree of conversion after n stages: 1	2	3	4
Co-current flow	250	2	8	0.25	0.46	0.63	0.77
Counter-current flow				0.24	0.45	0.62	0.76
UCM-model				0.24	0.45	0.62	0.75
Co-current flow	250	4	16	0.46	0.77		
Counter-current flow				0.46	0.78		
UCM-model				0.45	0.75		
Co-current flow	500	4	8	0.25	0.45	0.64	0.76
Counter-current flow				0.25	0.44	0.64	0.74
UCM-model				0.24	0.42	0.62	0.72

tion system. These data have been calculated for a representative set of parameter values.

From the numerical results shown in Table 2 it cannot only be concluded that the degree of conversion is quite unaffected by the relative flow direction of the mobile phases, but also that the superficial contact time, rather than the reactor height or superficial gas velocity, determines the degree of conversion reached. Moreover, it can be seen that the filter performance is hardly influenced by the number of individual stages a reactor system has been built up with, as long as a constant total height and thus a constant overall superficial gas contact time H_{total}/u_g is maintained.

As the trickling filter efficiency is quite independent of the relative flow direction of the gas phase, a further simplification of the system seems plausible, which assumes no concentration gradients to exist in the liquid phase at all. Although this liquid flow is of the plug flow type, it is regarded as ideally mixed with respect to the liquid concentration, a situation which can only be reached theoretically at infinite liquid velocity. This model will further be referred to as the U(niform) C(oncentration) M(odel).

A mathematical analysis of this mode of operation is presented in the Appendix, while some numerical results are shown in Table 2. From the analytical solution presented, it can directly be concluded that the degree of conversion is determined by the superficial contact time τ.

Appendix

If the overall reactor balance is applied instead of Eqs. (10, 11), it follows with Eqs. (8, 9):

$$u_g(C_{go}-C_{gH}) = K_0\,\delta\,a_w\,H\,\eta \tag{A.1}$$

or in dimensionless parameters:

$$1-C_g^*(1) = N_r\,\eta \tag{A.2}$$

Integration of Eq. (9) gives:

$$C_g^*(\xi) = C_l^* + (1-C_l^*)\exp\{-N_{og}\,\xi\} \tag{A.3}$$

Substitution of (A.2) into (A.3) for $\xi=1$ results in the following square-root equation:

$$C_l^* + \frac{N_r}{(1-\exp\{-N_{og}\})(C_{lcr}^*)^{1/2}}\,C_l^{*1/2} - 1 = 0 \tag{A.4}$$

The liquid concentration can be calculated from this equation as:

$$C_l^* = [-K^* + ((K^*)^2+1)^{1/2}]^2 \tag{A.5}$$

where

$$K^* = \frac{N_r}{2(C_{lcr}^*)^{1/2}(1-\exp\{-N_{og}\})}.$$

The effectiveness factor can now be calculated using Eq. (7b).

$$\eta = -K_1^* + [(K_1^*)^2 + K_2^*]^{1/2} \tag{A.6}$$

where

$$K_1^* = \frac{N_r}{2\,C_{lcr}^*(1-\exp\{-N_{og}\})};\quad K_2^* = \frac{1}{C_{lcr}^*}.$$

The elimination capacity follows from Eq. (A.6) as:

$$EC = EC_{\max}\,\eta \tag{A.7}$$

As the degree of conversion is defined by the ratio of the elimination capacity and the organic load to the system, it can be written as:

$$f = \frac{EC}{OL} = \frac{EC_{\max}\,H\,\eta}{u_g\,C_{go}} = \eta\,N_r \tag{A.8}$$

where both N_r and OL are linearly related to the superficial contact time τ.

Received July 13, 1990

R. M. M. Diks
S. P. P. Ottengraf
Department of Chemical Engineering
Laboratory of Chemical Process Technology
Eindhoven University of Technology
P.O. box 513
5600 MB Eindhoven
The Netherlands